arXiv:2103.11125v1 [stat.AP] 20 Mar 2021

Abstract

Crowd-sourcing has become a promising way to build a feature-based indoor positioning system that has lower labour and time costs. It can make full use of the widely deployed infrastructure as well as built-in sensors on mobile devices. One of the key challenges is to generate the reference feature map (RFM), a database used for localization, by aligning crowd-sourced trajectories according to associations embodied in the data. In order to facilitate the data fusion using crowd-sourced inertial sensors and radio signals, this paper proposes an approach to adaptively mining geometric information. This is the essential for generating spatial associations between trajectories when employing graph-based optimization methods. The core idea is to estimate the functional relationship to map the similarity/dissimilarity between radio signals to the physical space based on the relative positions obtained from inertial sensors and their associated radio signals. Namely, it is adaptable to different modalities of data and can be implemented in a self-supervised way. We verify the generality of the proposed approach through comprehensive experimental analysis: i) qualitatively comparing the estimation of geometric mapping models and the alignment of crowd-sourced trajectories; ii) quantitatively evaluating the positioning performance. The 68% of the positioning error is less than 4.7 m using crowd-sourced RFM, which is on a par with manually collected RFM, in a multi-storey shopping mall, which covers more than 10, 000 m^2.

Keywords: geometric constraint, sensor fusion, crowd-sourcing, graph optimization, feature-based indoor positioning

Mining geometric constraints from crowd-sourced radio signals and its application to indoor positioning

CAIFA ZHOU, ZHI LI, DANDAN ZENG, YONGLIANG WANG*

February 28, 2022

1 Introduction

Benefiting from the emergence and popularity of mobile devices and wireless communication networks, indoor positioning services with low-cost and sufficient accuracy become possible. Mobile devices play the role of receivers, and can observe various measurements (e.g., GNSS, IMU data, signals from Wi-Fi/BLE beacons) to indicate the location-relevant information of pedestrians. Wireless communication networks provide a large coverage of location-relevant signals in the environment without additional expense. One promising way to build such an indoor positioning system (IPS) is per crowd-sourcing which can obtain data without the explicit participation of pedestrians. In this way, it can make full use of the large number of in-use mobile devices and the existence of abundant location-relevant signals. Through the crowd-sourcing process, the goal is to construct a reference feature map (RFM), which includes the location and its corresponding location-relevant features, and can be applied to determine the location of pedestrians in the online phase.

In the case of passively crowd-sourcing relevant data to build an IPS, the main challenge is how to integrate collected data from multiple contributors at different times, which is equivalent to simultaneously localizing mobile devices and generating a (feature) map of the environment (i.e., SLAM) [1]. The process of RFM generation has to tackle the problem of multi-modalities originated from devices (i.e., hardware), pedestrian motions, and signal sources [2,3]. Among previous proposals [4–13], one promising approach to achieving data fusion is trajectory alignment [1] via graph-based optimization by identifying data associations (i.e., loop closures) contained in the crowd-sourced data.

When employing graph-based optimization for aligning multi-trajectories obtained per crowd-souring, it consists two ends: i) a front-end used to construct associations, which represent the spatial-temporal connectivity naturally embedded in measurable signals; and ii) a back-end to find the optimal alignment between multi-trajectories via minimizing a given loss function. Several well-known open-source software, such as g^{2}o [14] and Ceres [15], can be utilized to perform the optimization. However, there is lack of a general approach to building data associations according to observations. The construction of spatial-temporal associations using radio-frequency (RF) measurements is more difficult than applying visual or range observations (e.g., camera, LiDAR) [16,17], because there is no well-defined model that can be used to constrain the geometric relationship be-

*Riemann Lab, 2012 Laboratories, Huawei Technologies Co., Ltd, Xi'an, China (e-mail: {zhoucaifa, lizhi110, zengdandan4, wangyongliang775}@huawei.com). Corresponding author: Caifa Zhou (e-mail: zhoucaifa@huawei.com).

[1]Herein trajectory alignment denotes the estimation of transformation matrix between associated trajectories. This term is borrowed from [6].

tween RF measurements. This paper focuses on automatically mining data associations, which denote geometric constraints between crowd-sourced traces.

In order to mitigate the challenge of fusing crowd-sourced data, we propose an approach to constructing the spatial constraints depending only on IMU values and other location-relevant signals (mainly from Wi-Fi and BLE signals). Both measurements are available in crowd-sourced data. For a given similarity measure between RF features, we estimate a mapping function to indicate the relationship between the similarity in feature space and the geometric distance in geographical space. The mapping function can be used to approximate both the distance between a pair measured radio signals and the level of uncertainty of the distance estimation. Both of them are then used to build the spatial associations between trajectories. The proposed approach is to fuse multi-trajectories per graph-based optimization in order to align relatively located trajectories. It yields a RFM, which can be applied to feature-based indoor positioning, with low-cost.

We summarize the main contributions of this paper as follows:

1. We propose an approach to adaptively modelling the geometric information embodied in radio signals in order to characterize the uncertainty of data associations in a self-supervised manner.

2. We present a framework that integrates crowd-sourced location-relevant features and dead reckoning information from various mobile devices for feature-based indoor positioning in unknown environments with large scale.

3. We evaluate our approach in multi-storey shopping malls with an area over 10,000 m^2 (per floor) in the way of commercialized crowd-sourcing, which does not require any interaction from data contributors.

In the following sections, we first give a brief overview on previous work regarding RFM construction and geometric constraints generation in the field of feature-based indoor positioning. This is then followed by a formal definition of the problem of information fusion formulated as graph-based optimization. In Sec. 4 we present the approach to adaptively modelling the geometric information using the relative locations and radio signals in detail. In order to validate the proposed method, a comprehensive data collection and experimental analysis have been carried out. Sec. 5 provides extensive evaluations and results. Finally in Sec. 6, we conclude the paper.

2 Related work

The main topic of this paper involves the information fusion using graph-based optimization per crowd-sourcing in order to build IPS in a low-cost (both in time and labour) manner. We mainly present the literature related to methods for generating RFM using RF measurements. More details regarding feature-based positioning approaches and for extracting relative poses from IMU can be found e.g., in [18, 19] and [20, 21], respectively.

2.1 RFM construction approaches

Fully-supervised In the early stage of building a feature-based IPS, RFM was created by manually marking the reference locations and measuring the RF measurements in stop-and-go manner [22, 23]. In [18], Zhou et al. introduced a high precision tracking system for obtaining the reference locations in order to collect data kinematically. These approaches yield highly accurate reference locations, however, they are time-costing and labour-intensive. These two drawbacks greatly hinder the widespread deployment of feature-based IPS.

Weakly-supervised Compared to fully-supervised approaches, weakly-supervised ones incorporate other information to simplify the data collection procedure. The authors in [24,25] illustrated a quick RFM creation method, which requires the site surveyor (or the contributor of the crowdsourcing) to put starting and ending points on the map of the indoor region of interest. The reference locations are interpolated by assuming that the surveyor is moving along a straight line. This can speed-up data collection but requires indoor maps as well as the explicit interaction from surveyors. Another way to reduce the labour for collecting the RFM is by combining fully-supervised methods with reconstruction algorithms. A sparse data collection is firstly performed in a fully-supervised way. The sparsely collected RFM is used to reconstruct a dense RFM either by spatial interpolation [26, 27], e.g., compressive sensing [26], Gaussian process regression [28] or by employing the path-loss model of the RF signals [29]. However, the former is constrained by the granularity of existing reference locations, and the latter requires to know the location of signal sources in prior and to estimate the parameters of the propagation model for each signal source in different indoor regions.

Unsupervised There are three types of approaches to marking the reference locations in an unsupervised manner: i) with the help of floor plan [30,31]; ii) with the help of moving robots [32,33]; and iii) automatic trajectory fusion [5,6,9–12]. In [30] and [31], the reference locations are estimated by matching RF measurements with geometric features (e.g., connectivity between rooms, corridors, and corners) of the floor plan. PinLoc [32] and Slide [33] employed automatically controlled robots to improve the efficiency of site survey. However, it either requires indoor maps or introduces extra hardware. For the trajectory fusion approaches, they combined relative pose information, mostly from IMU, with constraints derived from measurable radio signals. The reference locations are obtained via solving an optimization problem. These methods are efficient and do not require additional support. However, they need to model constraints between RF measurements.

Our proposal is in an unsupervised manner. In contrast to previous work, our approach does not require any known reference locations as landmarks nor the help of dedicated surveying devices and detailed indoor maps.

2.2 Geometric constraints generation

When using graph-based optimization approaches to fuse the trajectories, the key is to build data associations. In [5, 6], Gu et al. proposed to build the RFM in a crowd-sourced way by aligning multi-trajectories using graph-based optimization. But it deployed the foot-mounted IMU, which can yield accurate relative pose estimations. Nowicki et al. [10,11] and Tan et al. [12] also employed graph optimization for aligning trajectories but it relies on known locations as landmarks to build the spatial relationship. These works employ a quasi-linear model to approximate the spatial constraints between trajectories using radio signals and cannot estimate the uncertainty of the geometric constraints. In addition, it requires priorly measured location of landmarks. In [9] authors employed the path-loss model for estimating the spatial relationship between relative locations. The main challenge of this approach is that parameters of the propagation model vary for each signal source as well as indoor environments. In [1], an approach based on similarity threshold between radio signals is used to detect data association. It utilizes the relative pose information to estimate the confidence (i.e., level of uncertainty) of data associations. However, it cannot model the expected distance between nodes but simply treats them at the same position if the similarity between radio signals is higher than the threshold. Compared to previous work, our proposal is in a self-supervised manner, namely modelling the geometric information (both the expected distance and its level of uncertainty) adaptively using the relative locations and their associated radio signals.

3 Information fusion as graph optimization

3.1 Representations

For one trajectory collected by crowd-sourcing contributors, it consists data from IMU and RF measurements. Each of the trajectory is used to extract relative spatial relationship according to IMU data, e.g., per traditional pedestrian dead reconking (PDR) [34] or learning-based approaches [20, 21]. Thus, the i-th trajectory $\mathbf{T}_i$ is represented using a sequence of relative positions and their associated observations, $\mathbf{T}_i = \{(x_i^{(k)}, y_i^{(k)}, \theta_i^{(k)}, \mathbf{O}_i^{(k)})\}$, where $x_i^{(k)}, y_i^{(k)}, \theta_i^{(k)}$ is the 2D pose (position plus heading) of the k-th location in a local coordinate frame of the trajectory, and $\mathbf{O}_i^{(k)}$ is the k-th observation associated to the corresponding location in case of opportunistic RF signals are measured. Without loss of generality, RF measurements from Wi-Fi/BLE beacons are taken as examples. Each RF observation consists a set of paired values, i.e., a unique identifier (e.g., MAC) and its corresponding value (e.g., received signal strength indicator or channel state information). Thus, the k-th observation $\mathbf{O}_i^{(k)}$ of i-th trajectory $\mathbf{T}_i$ is denoted as $\mathbf{O}_i^{(k)} := \{a : v | \mathbf{O}_i^{(k)}(a) = v, a \in \mathcal{A}_i^{(k)}\}$, where $\mathcal{A}_i^{(k)}$ is a set of identifiers of measurable signals.

In this paper, we represent the trajectory alignment as a graph-based optimization problem, in which the node $\mathbf{p} := (x, y, \theta)$ is the 2D pose of the contributors, and the edge $e_{ij}(\mathbf{p}_i, \mathbf{p}_j | \mathbf{O}_i, \mathbf{O}_j) := e_{ij}$ used to link these nodes is either from IMU measurements (temporal constraints) or from radio signals associated with each node (geometric constraints). The goal of trajectory alignment is to estimate the transformation matrix between associated nodes in order to transform all trajectories into a common coordinate frame. The approach to achieving such a goal is via minimizing a defined loss function associated with all edges.

3.2 Energy function and its minimization

An observation model h, denoting the function that builds edges between observations, is used to model expected observations for updating the nodes, $\mathbf{z} = h(\mathbf{p}) + \epsilon$, where $\epsilon \in \mathcal{N}(0, \Omega^{-1})$. The gap between modelled observations and expected ones denotes the error term that needs be minimized via the optimization. Following [14], the error function defined as negative log-likelihood of Gaussian priors can be formulated as a non-linear least squares (NLS) problem:

$$\hat{\mathbf{P}} = \underset{\mathbf{P}}{\operatorname{argmin}} (\sum_i \| h(\mathbf{p}_i) - \mathbf{z}_i \|_{\Omega_i}^2) \tag{1}$$

The above NLS problem can be solved efficiently using well-established solvers, e.g., Gauss-Newton, or Levenberg-Marquardt per gradient descent and it can be carried out via open-source libraries, such g^{2}o and Ceres. More details regarding graph-based optimization can be found e.g., in [6,11,14].

3.3 Temporal spatial association from IMU measurements

As presented in above section, the key to formulating the information fusion problem as graph-based optimization is to build associations between nodes. In this paper, we mainly take two types of edges into account: i) (local) temporal constraints between sequential positions obtained using IMU data; and ii) (global) geometric constraints between arbitrary positions from the RF measurements. The former type only exists intra-trajectory between consecutive nodes and the latter can be establish in both intra-/inter-trajectories. In order to build each type of edges, an observation function has to be provided for computing the expected measurements and its uncertainty.

For the local spatial association, we follow [5, 6] and formulate it as motion control input from inertial navigation system (INS). The observation model h^{IMU} extracts the motion control input $\mathbf{z}_{i+1}^{\text{IMU}}$ from a given pair of sequential nodes, $\mathbf{p}_i$ and $\mathbf{p}_{i+1}$, within one trajectory, i.e. $\mathbf{z}_{i+1}^{\text{IMU}} = h^{\text{IMU}}(\mathbf{p}_i, \mathbf{p}_{i+1}) + \epsilon_{i,i+1}^{\text{IMU}}$, where

$$h^{\text{IMU}}(\mathbf{p}_i, \mathbf{p}_{i+1}) = \begin{bmatrix} \cos(\theta_i) & -\sin(\theta_i) & 0 \\ \sin(\theta_i) & \cos(\theta_i) & 0 \\ 0 & 0 & 1 \end{bmatrix} \Delta\mathbf{p}_{i,i+1} \tag{2}$$

$$\Delta\mathbf{p}_{i,i+1} = \begin{bmatrix} x_i - x_{i+1} \\ y_i - y_{i+1} \\ \theta_i - \theta_{i+1} \end{bmatrix} \tag{3}$$

and $\epsilon_{i,i+1}^{\text{IMU}} \in \mathcal{N}(0, (\Omega_{i,i+1}^{\text{IMU}})^{-1})$, where

$$\Omega_{i,i+1}^{\text{IMU}} = \begin{bmatrix} a & 0 & 0 \\ 0 & a & 0 \\ 0 & 0 & b \end{bmatrix}. \tag{4}$$

The expected control input is obtained according to an INS calculated using IMU measurements and current control input is computed per optimized value of nodes. The information matrix in (4) is related to performance of the INS. In this paper, we adopt the state-of-the-art learning-based approach, *RoNIN* [20], for inferring the relative position. The value of coefficients a and b are set to 500 and 70, respectively. In this way, the information matrix does not take the diversity of devices and motions into account. Diversity consideration is relevant to improving the generality and is left for the future work.

3.4 System framework

Fig. 1 illustrates the proposed solution for generating RFM using crowd-sourced trajectories. It starts with crowd-sourcing raw measurements, including IMU readings and radio signals, from various mobile devices. These raw data are processed on a server. Relative poses are extracted per learning-based dead reckoning approach using IMU measurements. Their corresponding radio signals are associated according to the temporal information. The core module is the geometric information modelling (presented in Sec. 4), which takes extracted relative positions and radio signals as input and approximate geometric constraints according to similarity between radio signals. The adaptively estimated model is then used to build loop closures between trajectories in order to form a properly connected graph. The RFM is obtained per optimizing the graph using well-established graph optimizers.

4 Spatial association construction using radio signals

Regarding the geometric constraints, they are constructed using RF measurements based on the fundamental assumption that different locations can be identified by measurable radio signals. However, mining global spatial associations from radio signals is difficult due to three factors: i) although the propagation of RF signals in free-space follows the log-path loss model, it is difficult to estimate the attenuation factor of each signal source in the indoor environment; ii) it requires the absolute location information to estimate the propagation model but it is not available in crowd-sourced

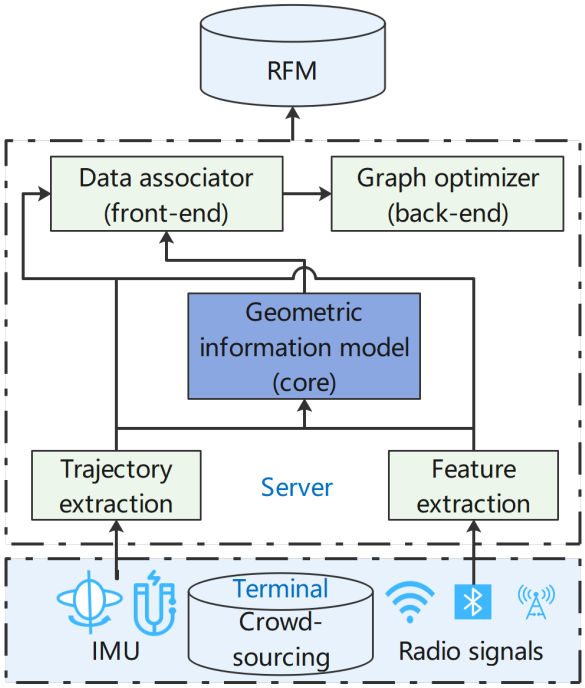
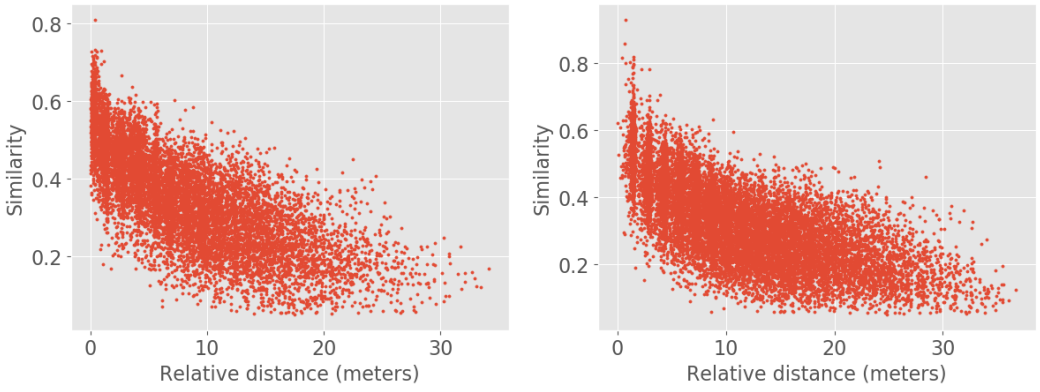


Figure 1: The scheme of proposed framework



(a) Example from test area 1

(b) Example from the test area 2

Figure 2: Examples of the relationship between similarity and distance

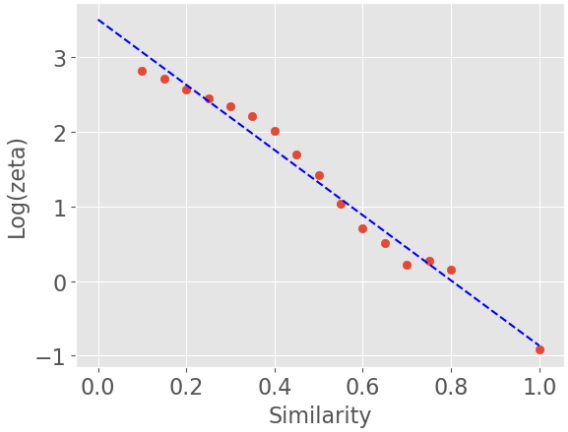


Figure 3: Example of log-linear relationship between ζ and similarity

trajectories; and iii) the estimation of the covariance matrix of RF measurements is complicated because the RF feature is in hyper-dimension.

Our proposal tackles the RF measurement-based association construction problem according to the findings that a proper metric g between radio signals can reflect the distance in geometric space. We downgrade the problem of estimating the observation model for each RF signal source at each location into a problem of approximating the spatial constraint according to the metric between each pair of RF measurements. In this way, it can make full use of the distance between relative positions inferred from IMU data.

Given a batch of crowd-sourced trajectories $\{\mathbf{T}_i\}_{i=1}^{M}$, a fix number of paired relative positions, which have the associated RF measurements, are arbitrarily sampled from each trajectory. It yields a set of paired positions and RF measurements $\mathbf{D} := \{(\mathbf{p}_i^{(l)}, \mathbf{p}_j^{(l)}, \mathbf{O}_i^{(l)}, \mathbf{O}_j^{(l)})\}_{l=1}^{N}$. These pairs are used to approximate the observation model h^{RF} to build the spatial constraints based on RF measurements such that:

$$z_{ij}^{\mathrm{RF}} = h^{\mathrm{RF}}(\mathbf{p}_i, \mathbf{p}_j, \mathbf{O}_i, \mathbf{O}_j | d, g) + \epsilon_{i,j}^{\mathrm{RF}} \tag{5}$$

where $\epsilon_{i,j}^{\mathrm{RF}} \in \mathcal{N}(0, (\sigma_{ij}^{\mathrm{RF}})^{-1})$. d and g are distance metrics between relative positions and similarity measure between RF measurements, respectively. Since to estimate the geometric information model using radio signals only requires information embodied in crowd-sourced trajectories, we can build geometric constraints in a fully-unsupervised (self-supervised) way. As the global spatial relationship is approximated according to the similarity measure, only the expected distance and its level of uncertainty is quantified. Namely, the spatial constrained between a pair of relative positions is defined on a circle in 2D-space (or a sphere in 3D-space). The proposed approach consists following key steps (summarized in Table 1):

- **Metric computing**: for each data point in $\mathbf{D}$, the distance between relative position and similarity measure are computed using the given d and g. In this paper, d is defined as Euclidean distance between x-y coordinates of $\mathbf{p}_i$ and $\mathbf{p}_j$. It represents the geometric distance by assuming the local consistency of the coordinate frame within one trajectory. The corresponding similarity between RF measurements is computed using a compound similarity measure, motivated by [35], which combines Jaccard similarity [36] and kernelized $\mathcal{L}_1$ similarity via

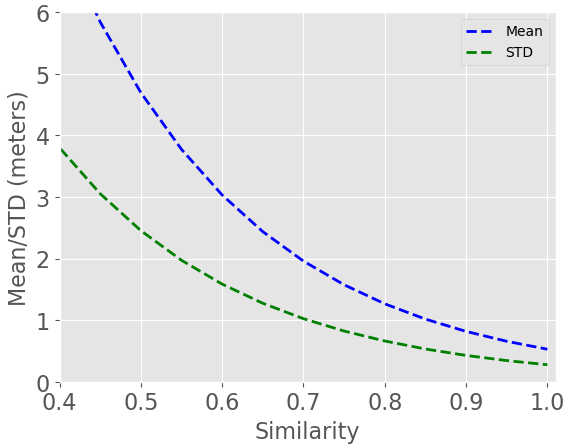


Figure 4: Example of fitted model of geometric constraints

harmonic mean (β-score):

$$g(\mathbf{O}_i, \mathbf{O}_j) = \frac{(1+\beta^2) \cdot g^{\text{Jac}}(\cdot,\cdot) \cdot g^{\text{L1}}(\cdot,\cdot)}{\beta^2 g^{\text{Jac}}(\cdot,\cdot) + g^{\text{L1}}(\cdot,\cdot)} \tag{6}$$

where $g^{\text{Jac}}(\cdot,\cdot)$ denotes the Jaccard similarity:

$$g^{\text{Jac}}(\mathbf{O}_i, \mathbf{O}_j) = \frac{|\mathcal{A}_i \cap \mathcal{A}_j|}{|\mathcal{A}_i \cup \mathcal{A}_j|}, \tag{7}$$

and $g^{\text{L1}}(\cdot,\cdot)$ is defined as mapping the average of $\mathcal{L}_1$ distance to a similarity measure using Gaussian kernel function:

$$g^{\text{L1}}(\mathbf{O}_i, \mathbf{O}_j) = \exp(-(\frac{\sum_{a \in \mathcal{A}_{ij}} (|v_i - v_j|)}{|\mathcal{A}_{ij}|})^2/(2\sigma^2)). \tag{8}$$

$\mathcal{A}_{ij} := \mathcal{A}_i \cup \mathcal{A}_j$. In case of $a \notin \mathcal{A}_i$ or $a \notin \mathcal{A}_j$, its corresponding value is set to a missing indicator. As both of the measured value of radio signals and estimated relative locations are affected by measurement noise, the relationship between distance and similarity is highly scattered as illustrated in Fig. 2.

- **Similarity binning**: According to (6), the similarity is in $[0, 1]$. In order to approximate the distribution of the geometric distance for a given similarity, a binning step is applied to divide the whole range into several bins with equal size. Each bin is denoted as $[c_i - \Delta, c_i + \Delta)$. The geometric distance whose corresponding similarity is within a given bin is assigned into the corresponding bin. Distances between relative positions lying in a certain bin are used to approximate the distribution.

- **Distribution approximating**: For each bin, we estimate the expected geometric distance and its uncertainty (i.e. standard deviation). We approximate its distribution under Rayleigh distribution assumption parametrized with ζ [37]. Under this assumption, the approximated

Table 1: Summary of the proposed approach

Inputs	A batch of trajectories $\{\mathbf{T}_i\}_{i=1}^{M}$
	Geometric distance metric d
	Similarity measure g
Output	$f : g(\mathbf{O}_i, \mathbf{O}_j) \mapsto \zeta$
1:	Sampling paired relative positions with RF measurements from each trajectory
2:	Computing the geometric distance and similarity measure for each pair of data points using the given d and g
3:	Binning the similarity range into C bins and assigning the geometric distance to the corresponding bins
4:	Estimating the parameter $\hat{\zeta}_i$ of the assumed Rayleigh distribution for each bin centred at similarity value c_i using kernel density estimators or maximum likelihood estimation
5:	Estimating the parameter of f per linear fitting under log-linear assumption using $\{c_i, \hat{\zeta}_i\}_{i=1}^{C}$

expected geometric distance and its variance is defined as:

$$\begin{aligned} \mu_d &= \zeta\sqrt{\frac{\pi}{2}} \\ \sigma_d^2 &= \frac{4-\pi}{2} \cdot \zeta^2 \end{aligned} \tag{9}$$

where ζ is the parameter for the Rayleigh distribution of the geometric distances in a given bin. The value of ζ is estimated via a density estimator (e.g., kernel density estimation [38]) owing to the fact that the maximum value of probability is achieved at the value of ζ when assumed as the Rayleigh distribution or maximum likelihood estimator [37].

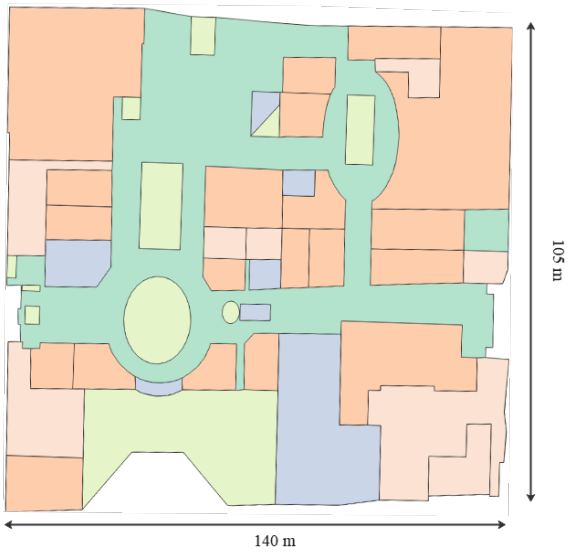
- **Parameter estimating**: Assuming that the similarity range is divided into C bins, we can have a set of paired the similarity and its distribution parameter $\{c_i, \hat{\zeta}_i\}_{i=1}^{C}$. From which, we would like to estimate a parametric model f such that given a similarity value $g(\mathbf{O}_i, \mathbf{O}_j)$, it maps to an estimated ζ value, i.e. $f : g(\mathbf{O}_i, \mathbf{O}_j) \mapsto \zeta$. Thus, the expected geometric distance and its variance can be calculated using (9). This parametric model is assumed as log-linear for avoiding negative approximation of ζ as well as the linearity between logarithm of ζ and the similarity as shown in Fig. 3. The parameters are obtained per linear fitting. These estimated parameters can be applied to infer geometric constraints in a continuous space (see Fig. 4).

5 Experimental analysis

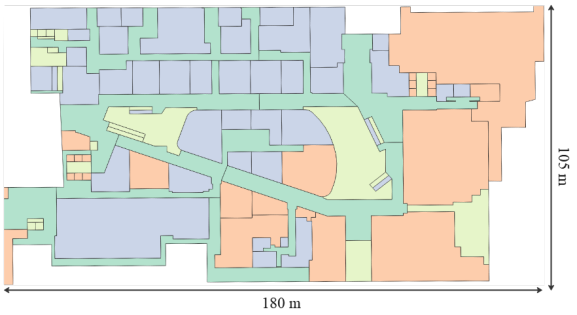
5.1 Experimental setup

5.1.1 Dataset

In order to evaluate the performance of proposed approach, the crowd-sourcing procedures have been carried out in two shopping malls illustrated in Fig. 5. Each of them consists multi-storey and each floor covers an area over 10,000 m^2. The data were collected by a custom-developed



(a) Floor plan of the test area 1



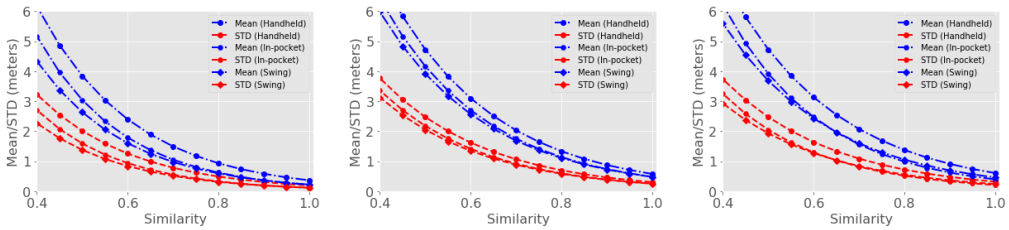
(b) Floor plan of the test area 2

Figure 5: Floor plan of test areas (Green parts indicate the accessible areas.)

application which can obtain readings from all built-in sensors of the mobile device. Without losing the generality, only radio signals from WiFi access points (BLE beacons are omitted but includes mobile hotspots) are used for building the data associations as well as for indoor positioning.

The crowd-sourcing is carried out using various type of mobile devices [2] by different volunteers without constraining walking poses (e.g., static hold or swing) and attachments of mobile devices (e.g., handheld or in-pocket). We denote the data collection as commercialized-crowd-sourcing (CCS). Although it requires volunteers to report their walking poses and attachment of mobile devices as well as roughly mark the area where they have crowd-sourced (e.g., the floor and passed-by accessible areas), these data are only used for the purpose of validation. Knowing the floor of each trajectory in advance is to reduce the influence of mis-identification of the traces' floor. Automatically identification of the floor of trajectories (or a bunch of traces) is relevant for generating the RFM. However, it is out-of-scope of this paper and left for future work.

[2]The crowd-sourcing is carried by recruiting beta-test participants among all Huawei mobile service users under their agreement.



(a) Test area 1 (F1) (b) Test area 1 (F3) (c) Test area 1 (F5)

Figure 6: Impact of walking poses on geometric information modelling

Table 2: Summary of collected data

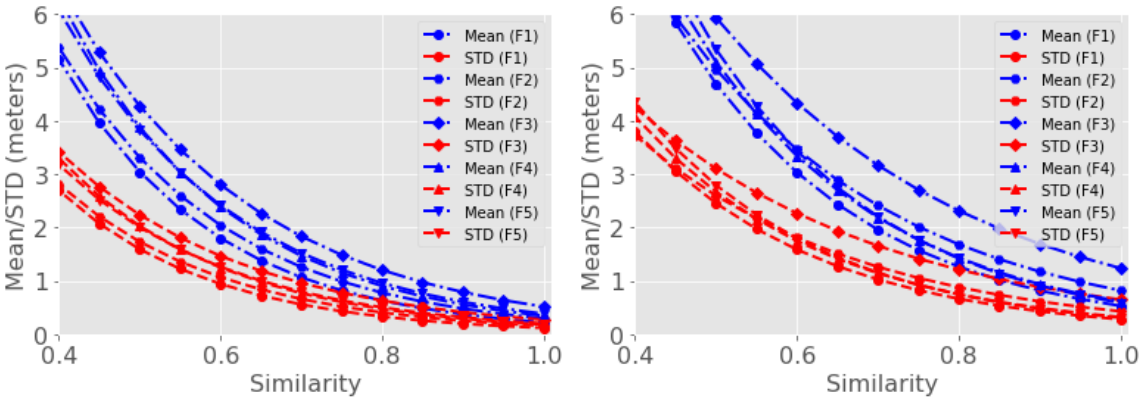
	Floor	CCS				MSS		Test dataset		Total APs
		♯ Traj.	Length (m)	♯ Samples	♯APs	♯Samples	♯APs	♯Samples	♯APs	
Test area 1	F1	89	1991	1149	1617	1098	2589	300	2112	2833
	F2	115	2093	1136	1597	1218	2792	290	2156	2942
	F3	135	2706	814	1578	807	2407	234	2159	2639
	F4	137	2804	1357	1657	837	2435	290	2099	2673
	F5	149	3502	1834	1637	821	2573	272	2043	2789
Test area 2	F1	121	2481	1698	1951	589	2363	341	1917	2958
	F2	63	1327	850	1544	773	2619	219	1839	3009
	F3	52	880	505	1274	517	1909	205	1454	2271
	F4	57	1055	648	1150	518	1555	234	1369	1867
	F5	61	1013	610	1025	662	1763	280	1253	2103

For quantitative evaluation of the positioning accuracy, we manually collected the RFM (denoted as manually site surveying (MSS)) and test points in both test areas using an unmanned ground vehicle, which is mounted with LiDAR and the mobile device. It is capable of performing visual-SLAM in centi-meter accuracy. The mapped test areas are used to obtain the reference locations and the ground truth of test points for evaluating the positioning performance. The detail information of collected data is summarized in Table 2 [3].

5.1.2 Short on positioning approach

After using graph-based optimization to align the crowd-sourced trajectories, all relative locations can be mapped into a common coordinate frame. These locations and their associated radio signals are used as the RFM for feature-based indoor positioning. Herein we employ k-nearest neighbour search [22, 36], a widely used deterministic feature-based positioning method, to evaluate the positioning performance. The distance metric used to match radio signals is defined as $1 - g(\mathbf{O}_i, \mathbf{O}_j)$ and the parameter k equals to 5 and 10 for test area 1 and 2 via grid search, respectively.

[3]The summary of APs takes all measured ones into account without e.g., identifying mobile APs or detecting changes of fixed APs.



(a) Test area 1

(b) Test area 2

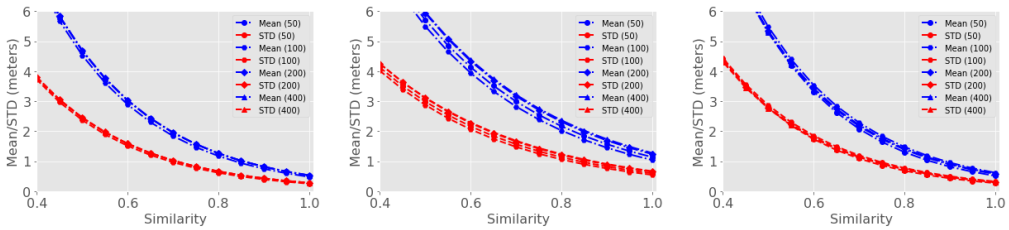
Figure 7: Impact of indoor regions on geometric information modelling

5.1.3 Evaluation metrics

For the geometric information modelling, we mainly evaluate and compare the generality qualitatively by modelling geometric constraints using different data sources, which are obtained in various walking poses, placement of mobile devices and indoor regions. In addition, we also evaluate the trajectory alignment qualitatively via visualizing it with the floor plan of indoor regions. Regarding the positioning performance, Euclidean distance between the estimate position and the corresponding ground truth is computed. The empirical cumulative distribution function (ECDF) of positioning error and its statistical values (e.g., circular error probable (CEP)) are used as the quantitative evaluation metrics.

5.2 Geometric constraint modelling

In order to validate the proposed approach to modelling the geometric constraints, we evaluated and compared geometric information modelling results in case of various walking poses, indoor regions and the number of sampled pairs. As shown in Fig. 6 the impact of walking poses on the estimated geometric constraints regarding the given value of the similarity varies over different indoor regions, however the range of the variation is limited, especially when the similarity is higher than 0.6. Regarding the impact of indoor regions, the results illustrated in Fig. 7 depict that the consistency of geometric constraint models is high in most indoor regions over different floors and buildings. It means that the pre-estimated model can be transferred from one indoor region to another for improving the generalizability. Compare to the impact of walking poses and indoor regions on the geometric modelling, the sampling of the paired relative position and RF measurement has much less influence as shown in Fig. 8. It reveals the characteristic of the robustness of the proposed approach against arbitrary sampling. In the following experimental analysis, the geometric model estimation is carried out using crowd-sourced trajectories for each floor with diverse walking poses. The resampling number is set to 100.



(a) Test area 2 (F1) (b) Test area 2 (F3) (c) Test area 2 (F5)

Figure 8: Impact of the number of sampled pairs on geometric information modelling

5.3 Trajectory fusion and indoor positioning

5.3.1 Qualitative evaluation of trajectory fusion

The trajectory fusion is achieved using graph optimization based on the open-source framework provided by g^{2}o and the data associations between relative locations are built according to the estimated geometric information model for each indoor region[4]. The key to aligning crowd-sourced trajectories is to build the spatial association between them. The number of generated edges between nodes is balanced by choosing the value of threshold on similarity between radio signals. Once data associations were established, graph-based optimization[5] can be employed to align relative trajectories into a common reference frame (following the procedures presented in Fig. 1). The value of the threshold determines the connectivity between trajectories. The higher the threshold on similarity, the less the number of edges between trajectories. We threshold the similarity from 0.05 to 0.95 with interval of 0.1. As presented in Fig. 9, we can obtain that there are too many false edges between trajectories, the crowd-trajectories are condensed too much when the threshold is small (e.g., 0.25). With a high threshold (e.g., 0.65), it results in low connectivity between trajectories, which cannot provide adequate geometric constraints for estimating the transformation matrix between them. Therefore, the crowd-sourced trajectories cannot be aligned properly. By performing the grid search, the suitable value of the threshold equals to 0.45 for both test areas.

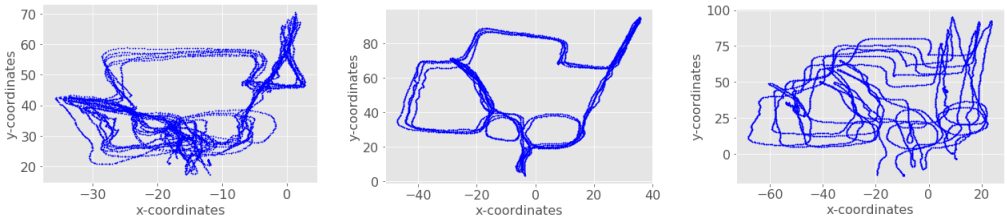
As shown in Fig. 10, the mis-aligned raw trajectories (1st column), which are in separate local reference frames, seem very noisy and without clear relations. After performing graph optimization according to the geometric constraints between different pairs of trajectories by thresholding on the similarity, these raw trajectories can be fused together and aligned properly into one common reference frame (2nd column). Qualitatively, these aligned trajectories are well-matched to the floor plan of the indoor region per manual projection as illustrated in 3rd column of Fig. 10.

5.3.2 Evaluation of positioning performance

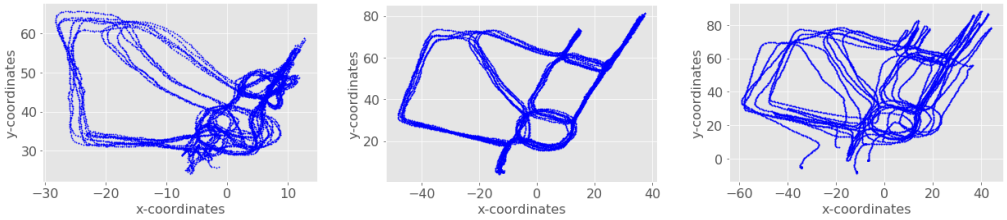
Employing the RFM generated per information fusion using the crowd-sourced trajectories or the RFM by site surveying, the location of pedestrian can be determined by matching online measured radio signals with them. The statistical positioning results of two test areas are presented in Table 3 and the ECDF of the positioning error is visualized in Fig. 11. Regarding floor identification accuracy, the overall accuracy is about 97% and 96% using crowd-sourced RFM in both test areas. Compared

[4] `https://github.com/RainerKuemmerle/g2o/tree/master/g2o`

[5] In the implementation of g^{2}o, a built-in edge pruning based robust kernels is also used to remove the false connections.

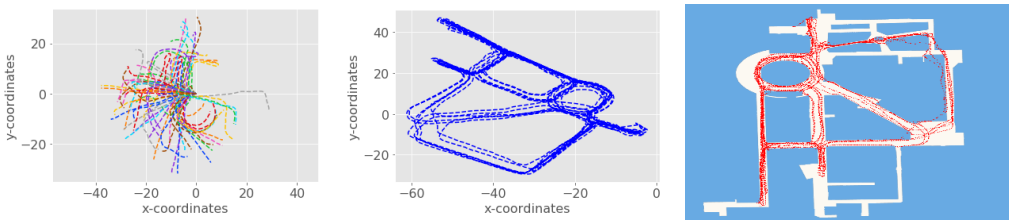


(a) 0.25 (b) 0.45 (c) 0.65

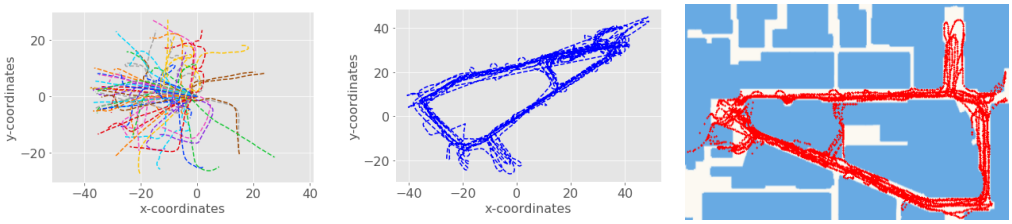


(d) 0.25 (e) 0.45 (f) 0.65

Figure 9: The impact of the threshold on trajectory alignment (Top: F3 of test area 1/Bottom: F5 of test area 1)



(a) Raw trajectories (b) Aligned trajectories (c) Aligned trajectories



(d) Raw trajectories (e) Aligned trajectories (f) Aligned trajectories

Figure 10: Qualitative evaluation of aligned trajectories (Top: F5 of test area 1/Bottom: F1 of test area 2)

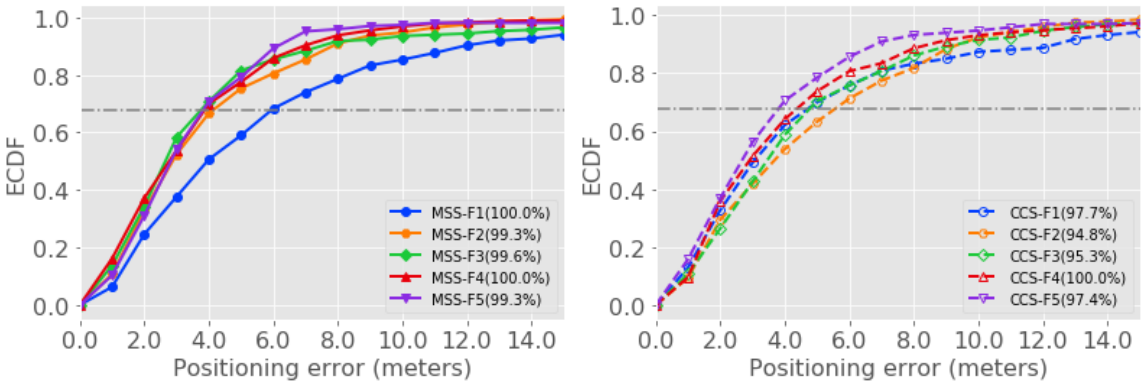
Table 3: Statistical of positioning performance

		Floor Acc. (%)		Positioning error (m)							
				Min.		Mean		CEP68		CEP95	
		MSS	CCS	MSS	CCS	MSS	CCS	MSS	CCS	MSS	CCS
Test area 1	F1	100	97.7	0.2	0.1	5.4	4.8	6.0	4.7	15.5	15.3
	F2	99.3	94.8	0.1	0.1	3.8	4.6	4.3	5.6	9.8	11.4
	F3	99.6	95.3	0.1	0.2	3.8	4.6	3.9	4.9	12.8	12.0
	F4	100	100	0.2	0.1	3.5	4.1	3.9	4.5	8.6	11.8
	F5	99.3	97.4	0.2	0.1	3.6	3.6	3.8	3.8	6.9	10.0
	Overall	99.6	97.0	0.2	0.1	4.0	4.3	4.4	4.7	10.7	12.1
Test area 2	F1	99.4	100	0.2	0.1	5.6	3.9	6.0	4.5	14.0	9.5
	F2	96.9	89.3	0.5	0.4	8.7	6.3	7.0	6.0	30.0	14.0
	F3	96.6	100	0.3	0.4	4.1	6.3	4.7	7.3	9.7	15.2
	F4	99.6	90.6	0.2	0.3	6.7	7.4	7.5	8.6	16.4	19.1
	F5	99.7	100	0.5	0.2	7.0	6.0	7.9	6.9	18.2	14.2
	Overall	98.4	96.0	0.3	0.3	6.4	6.0	6.6	6.7	17.7	14.4

to the floor detection accuracy using the RFM by MSS, the retreat is only 2 percentage point. For the location-wise positioning performance, the mean positioning error and CEP68 using crowd-sourced RFM are on a par with that using manually collected RFM in both test areas. The mean positioning error in test area 1 using CCS RFM is 4.3 meters, which falls back only 0.3 meters comparing to that of using MSS RFM. As in test area 2, the mean positioning error using CCS RFM is decreased by 0.4 meters when comparing using MSS RFM, whose mean positioning error is 6.4 meters.

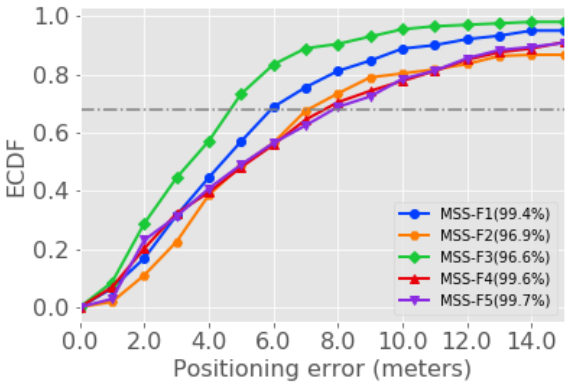
6 Conclusion

In this paper, we propose an approach for adaptively modelling the geometric information in a self-supervised manner using the crowd-sourced relative locations (e.g., from inertial sensors or vision-inertial odometer) and their associated radio signals. The key to building the model is to map the similarity between radio signals to the physical distance under the assumption of Rayleigh distribution. Geometric constraints obtained from radio signals can be used to fuse crowd-sourcing trajectories per solving an optimization problem. Through comprehensive experimental analysis, we validate the generalizability of the proposed approach and its applicability to trajectory alignment, which can generate the RFM for feature-based indoor positioning. Using the RFM generated from the crowd-sourced trajectories, the average floor identification accuracy is over 96%, which is on a par with the one using manually collected RFM. The retreat is only about 2 percentage point. The mean positioning error is about 4.3 meters and 6.0 meters using crowd-sourced RFM in test area 1 and area 2, respectively. This is at the same level of using site surveyed RFM. In order to alleviate the limitations of our proposal, the continuative research would focus on: i) the quantification of the uncertainty of relative positions obtained from IMU measurements; ii) the adaptiveness to long-term variations and device diversities; and iii) refinement of the crowd-sourced RFM.

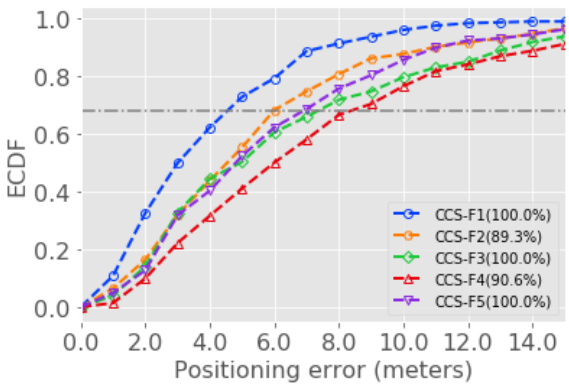


(a) MSS

(b) CCS



(c) MSS



(d) CCS

Figure 11: ECDF of the positioning results (Top: Test area 1/Bottom: Test area 2). Number in the bracket denotes the floor identification accuracy. The dashed grey line in each figure indicates the CEP68.

Acknowledgment

The authors would like to thank the contribution of group members of positioning team at Riemann Lab, 2012 Laboratories, especially to Dr. Yun Zhang, Dr. Ran Guan, Xiya Cao, Jiaming Chen, and Mengchao Li, for their help of data processing and valuable discussions. Furthermore, we would like to thank the work of peer-reviews. Their suggestions have largely improve the quality of this paper.

References

[1] R. Liu, S. H. Marakkalage, M. Padmal, T. Shaganan, C. Yuen, Y. L. Guan, and U.-X. Tan, "Collaborative slam based on wifi fingerprint similarity and motion information," *IEEE Internet of Things Journal*, vol. 7, no. 3, pp. 1826–1840, 2019.

[2] X. Zhu, W. Qu, T. Qiu, L. Zhao, M. Atiquzzaman, and D. O. Wu, "Indoor intelligent fingerprint-based localization: Principles, approaches and challenges," *IEEE Communications Surveys & Tutorials*, vol. 22, no. 4, pp. 2634–2657, 2020.

[3] B. Wang, Q. Chen, L. T. Yang, and H.-C. Chao, "Indoor smartphone localization via fingerprint crowdsourcing: Challenges and approaches," *IEEE Wireless Communications*, vol. 23, no. 3, pp. 82–89, 2016.

[4] C. Wu, Z. Yang, and Y. Liu, "Smartphones based crowdsourcing for indoor localization," *IEEE Transactions on Mobile Computing*, vol. 14, no. 2, pp. 444–457, 2014.

[5] Y. Gu, C. Zhou, A. Wieser, and Z. Zhou, "Wifi based trajectory alignment, calibration and crowdsourced site survey using smart phones and foot-mounted imus," in *2017 International Conference on Indoor Positioning and Indoor Navigation (IPIN)*, pp. 1–6, 2017.

[6] Y. Gu, C. Zhou, A. Wieser, and Z. Zhou, "Trajectory estimation and crowdsourced radio map establishment from foot-mounted imus, wi-fi fingerprints, and gps positions," *IEEE Sensors Journal*, vol. 19, no. 3, pp. 1104–1113, 2019.

[7] Z. Li, X. Zhao, and H. Liang, "Automatic construction of radio maps by crowdsourcing pdr traces for indoor positioning," in *2018 IEEE International Conference on Communications (ICC)*, pp. 1–6, IEEE, 2018.

[8] S. Yang, P. Dessai, M. Verma, and M. Gerla, "Freeloc: Calibration-free crowdsourced indoor localization," in *2013 Proceedings IEEE INFOCOM*, pp. 2481–2489, 2013.

[9] Z. Zuo, L. Liu, L. Zhang, and Y. Fang, "Indoor positioning based on bluetooth low-energy beacons adopting graph optimization," *Sensors*, vol. 18, no. 11, 2018.

[10] M. Nowicki and P. Skrzypczyński, "Indoor navigation with a smartphone fusing inertial and wifi data via factor graph optimization," in *International Conference on Mobile Computing, Applications, and Services*, pp. 280–298, Springer, 2015.

[11] M. R. Nowicki and P. Skrzypczyński, "A multi-user personal indoor localization system employing graph-based optimization," *Sensors*, vol. 19, no. 1, p. 157, 2019.

[12] J. Tan, X. Fan, S. Wang, and Y. Ren, "Optimization-based wi-fi radio map construction for indoor positioning using only smart phones," *Sensors*, vol. 18, no. 9, p. 3095, 2018.

[13] Z. Li, X. Zhao, Z. Zhaoa, and T. Braun, "Wifi-rita positioning: Enhanced crowdsourcing positioning based on massive noisy user traces," *IEEE transactions on wireless communications*, 2021.

[14] G. Grisetti, R. Kümmerle, H. Strasdat, and K. Konolige, "g2o: A general framework for (hyper) graph optimization," in *Proceedings of the IEEE International Conference on Robotics and Automation (ICRA), Shanghai, China*, pp. 9–13, 2011.

[15] S. Agarwal, K. Mierle, and Others, "Ceres solver." `http://ceres-solver.org`.

[16] T. Taketomi, H. Uchiyama, and S. Ikeda, "Visual slam algorithms: a survey from 2010 to 2016," *IPSJ Transactions on Computer Vision and Applications*, vol. 9, no. 1, pp. 1–11, 2017.

[17] C. Cadena, L. Carlone, H. Carrillo, Y. Latif, D. Scaramuzza, J. Neira, I. Reid, and J. J. Leonard, "Past, present, and future of simultaneous localization and mapping: Toward the robust-perception age," *IEEE Transactions on robotics*, vol. 32, no. 6, pp. 1309–1332, 2016.

[18] C. Zhou, *Mitigating Variability Issues for Feature-based indoor positioning.* PhD thesis, ETH Zurich, 2019.

[19] S. He and S. . G. Chan, "Wi-fi fingerprint-based indoor positioning: Recent advances and comparisons," *IEEE Communications Surveys Tutorials*, vol. 18, no. 1, pp. 466–490, 2016.

[20] H. Yan, S. Herath, and Y. Furukawa, "Ronin: Robust neural inertial navigation in the wild: Benchmark, evaluations, and new methods," *arXiv preprint arXiv:1905.12853*, 2019.

[21] W. Liu, D. Caruso, E. Ilg, J. Dong, A. I. Mourikis, K. Daniilidis, V. Kumar, and J. Engel, "Tlio: Tight learned inertial odometry," *IEEE Robotics and Automation Letters*, vol. 5, no. 4, pp. 5653–5660, 2020.

[22] P. Bahl and V. N. Padmanabhan, "Radar: An in-building rf-based user location and tracking system," in *Proceedings IEEE INFOCOM 2000. Conference on Computer Communications. Nineteenth Annual Joint Conference of the IEEE Computer and Communications Societies (Cat. No. 00CH37064)*, vol. 2, pp. 775–784, Ieee, 2000.

[23] M. Youssef and A. Agrawala, "The horus wlan location determination system," in *Proceedings of the 3rd international conference on Mobile systems, applications, and services*, pp. 205–218, 2005.

[24] H.-H. Liu and C. Liu, "Implementation of wi-fi signal sampling on an android smartphone for indoor positioning systems," *Sensors*, vol. 18, no. 1, p. 3, 2018.

[25] H.-H. Liu, "The quick radio fingerprint collection method for a wifi-based indoor positioning system," *Mobile Networks and Applications*, vol. 22, no. 1, pp. 61–71, 2017.

[26] C. Feng, W. S. A. Au, S. Valaee, and Z. Tan, "Received-signal-strength-based indoor positioning using compressive sensing," *IEEE Transactions on mobile computing*, vol. 11, no. 12, pp. 1983–1993, 2011.

[27] A. Khalajmehrabadi, N. Gatsis, D. J. Pack, and D. Akopian, "A joint indoor wlan localization and outlier detection scheme using lasso and elastic-net optimization techniques," *IEEE Transactions on Mobile Computing*, vol. 16, no. 8, pp. 2079–2092, 2016.

[28] M. M. Atia, A. Noureldin, and M. J. Korenberg, "Dynamic online-calibrated radio maps for indoor positioning in wireless local area networks," *IEEE Transactions on Mobile Computing*, vol. 12, no. 9, pp. 1774–1787, 2012.

[29] O. Belmonte-Fernandez, R. Montoliu, J. Torres-Sospedra, E. Sansano-Sansano, and D. Chia-Aguilar, "A radiosity-based method to avoid calibration for indoor positioning systems," *Expert Systems With Applications*, vol. 105, pp. 89–101, 2018.

[30] C. Wu, Z. Yang, Y. Liu, and W. Xi, "Will: Wireless indoor localization without site survey," *IEEE Transactions on Parallel and Distributed Systems*, vol. 24, no. 4, pp. 839–848, 2012.

[31] G. Shen, Z. Chen, P. Zhang, T. Moscibroda, and Y. Zhang, "Walkie-markie: Indoor pathway mapping made easy," in *Presented as part of the 10th {USENIX} Symposium on Networked Systems Design and Implementation ({NSDI} 13)*, pp. 85–98, 2013.

[32] S. Sen, B. Radunovic, R. R. Choudhury, and T. Minka, "You are facing the mona lisa: Spot localization using phy layer information," in *Proceedings of the 10th international conference on Mobile systems, applications, and services*, pp. 183–196, 2012.

[33] K. Chen, C. Wang, Z. Yin, H. Jiang, and G. Tan, "Slide: Towards fast and accurate mobile fingerprinting for wi-fi indoor positioning systems," *IEEE Sensors Journal*, vol. 18, no. 3, pp. 1213–1223, 2018.

[34] R. Hostettler and S. Särkkä, "Imu and magnetometer modeling for smartphone-based pdr," in *2016 International Conference on Indoor Positioning and Indoor Navigation (IPIN)*, pp. 1–8, IEEE, 2016.

[35] C. Zhou and A. Wieser, "Cdm: Compound dissimilarity measure and an application to fingerprinting-based positioning," in *2018 International Conference on Indoor Positioning and Indoor Navigation (IPIN)*, pp. 1–7, IEEE, 2018.

[36] C. Zhou and A. Wieser, "Modified jaccard index analysis and adaptive feature selection for location fingerprinting with limited computational complexity," *Journal of Location Based Services*, vol. 13, no. 2, pp. 128–157, 2019.

[37] D. Roy, "Discrete rayleigh distribution," *IEEE Transactions on Reliability*, vol. 53, no. 2, pp. 255–260, 2004.

[38] J. Kim and C. D. Scott, "Robust kernel density estimation," *The Journal of Machine Learning Research*, vol. 13, no. 1, pp. 2529–2565, 2012.